Synthesis of colloidal nanoparticles during femtosecond laser ablation of gold in water

A. V. Kabashin[a] and M. Meunier
Laser Processing Laboratory, Department of Engineering Physics, Ecole Polytechnique de Montréal, Case Postale 6079, succ. Centre-ville, Montréal (Québec), H3C 3A7 Canada

(Received 5 August 2003; accepted 24 September 2003)

Femtosecond laser radiation has been used to ablate a gold target in pure deionized water to produce colloidal gold nanoparticles. We report evidence for two different mechanisms of material ablation in the liquid environment, whose relative contributions determine the size distribution of the produced particles. The first mechanism, associated with thermal-free femtosecond ablation, manifests itself at relatively low laser fluences $F<400$ J/cm^2 and leads to very small (3–10 nm) and almost monodispersed gold colloids. The second one, attributed to the plasma-induced heating and ablation of the target, takes place at high fluences and gives rise to a much larger particle size and broad size distribution. The fabricated nanoparticles exhibit plasmon-related optical absorption peak and are of significance for biosensing applications. © *2003 American Institute of Physics.*
[DOI: 10.1063/1.1626793]

Remarkable size-dependent optical properties of colloidal gold nanoparticles related to the generation of Mie resonances[1] and to quantum size effects[2] make them very attractive for intensive research and different applications in biotechnology. In particular, being linked to biological objects, these nanoparticles can serve as efficient optical markers to screen selective biointeractions. 10–30 nm gold colloids with relatively narrow size dispersion are generally fabricated by a chemical method, in which a diluted metal salt is reduced in an aqueous solution with a reducing reagent.[3] However, this chemical method is not free of contamination byproducts, which complicate further stabilization of the colloidal solution and functionalization of the gold surface for biological immobilizations.

Laser-induced ablation from a solid target is known as an alternative physical method for nanofabrication. Being performed in a controllable contamination-free environment this method makes possible the production of nanomaterials without impurities. In particular, laser ablation of silicon in inert gases was previously used to produce Si nanoclusters,[4,5] which were then deposited on a substrate to form nanostructured films.[6–9] On the other hand, one can effectively produce colloidal metal nanoparticles when the ablation occurs in a liquid environment.[10,11] However, the laser ablation in pure water generally gives relatively large (20–300 nm) and strongly dispersed (50–300 nm) particles[12–18] due to both the postablation agglomeration of nanoclusters and to the ejection of large target fragments, although certain size control can be achieved by a variation of radiation parameters.[12,16] It has been recently demonstrated[12–14] that the nanoparticle size can be drastically reduced by the use of aqueous solutions of surfactants, which cover the particles just after their ablation and thus prevent them from further agglomeration. Sodium dodecyl sulfate (SDS) was found to be the most efficient among the surfactants to reduce the mean size of Au nanoparticles down to 5 nm during nanosecond laser ablation of gold.[13] Ablating a gold target by femtosecond radiation in aqueous solutions of cyclodextrins (torus-like macrocycles built up from glucose pyranose units[19]), we recently demonstrated a formation of gold nanoparticles with the mean size and dispersion of 2 and 1 nm, respectively.[18] In contrast to surfactants, cyclodextrins should not terminate the surface and keep it useful for further (bio-) chemical modifications. However, physical aspects of laser ablation in liquids still remain unclear and relative contributions of the physical and chemical factors of particle reduction have not yet been well understood.

In this communication, we study physical mechanisms for the nanoparticle size control during the femtosecond laser ablation in liquids. In particular, we report the fabrication of very small and almost monodispersed particles in the absence of any reducing chemical reagents.

The experiments were carried out with a Ti/sapphire laser (Hurricane, Spectra Physics Lasers), which provided 110 fs full width at half maximum (FWHM) pulses (wavelength 800 nm, maximum energy 1 mJ/pulse, repetition rate of 1 kHz). The radiation was focused by an objective with the focal distance of 7.5 cm on the top of a gold rod (99.99%) with the height of 1.5 mm and diameter of 6 mm, which was placed on the bottom of a 2-mL-glass vessel filled with pure 18 MΩ deionized water. The thickness of the water layer above the rod was 10 mm. The vessel was placed on a horizontal platform, which executed repetitive circular motions at a constant speed of 0.5 mm/s to form circle-like ablated region on the target surface. For all samples, the ablation was performed during 20 min. A transmission electron microscope (TEM) with 0.23 nm point–point resolution (model Philips CM30) was used to take electron images of the nanoparticles in the solution. A drop of a sample solution was placed on a carbon-coated copper grid and then dried at room temperature. Normally, the diameters of 1000 particles were measured and the particle size (diameter) distribution was obtained. Target surface was examined by scanning elec-

[a]Electronic mail: andrei.kabashin@polymtl.ca

tron microscopy [(SEM), model Phillips XL20]. In addition, we recorded absorption spectra in the 250–1000 nm range using a Lambda 19 Spectrometer (Perkin Elmer).

The laser ablation of gold in water was accompanied by the presence of a plasma plume on the target surface, easily visible by the naked eye. The plasma plume intensity depended on the laser energy and light focusing conditions. In contrast to the ablation in residual gases,[4–9] the focusing conditions were determined not only by the target position with respect to the focusing lens, but also by the thickness of the water layer above the gold surface. This was apparently connected to a certain shift of the focal plane due to the water optical refraction. In the experiments, identical focusing conditions were maintained by fixing both the target–lens distance and the water thickness, while the radiation energy was the main variable parameter to control the laser fluence. The material ablation threshold was estimated by examining the craters on the target.[20] This threshold was found to be at least fivefold higher for water compared to vacuum ($F \sim 1$ J/cm^2). Note that a similar difference of femtosecond ablation efficiencies was recently recorded for silver.[17]

We observed a visible coloration of the solution after several seconds of the experiment. The color of solutions prepared at low fluences $F < 100$ J/cm^2 was red or pink, whereas the solution prepared at high fluences $F > 100$ J/cm^2 looked red-violet with some yellow tint. In the absorption spectra of the solutions, the surface plasmon-related peak could be clearly distinguished. This peak was around 520–530 nm for $F < 100$ J/cm^2, which was consistent with the presence of small 3–30 nm particles in the solution.[1,2] However, for $F > 100$ J/cm^2, the peak suffered a broadening and a red shift to 540–550 nm, suggesting a certain ''dephasing'' of signals from individual plasmons due to the increase of particle size and dispersion.[2] The hypothesis on the fluence dependence of the nanoparticle size was confirmed by TEM data, which revealed a drastic particle size reduction under the laser fluence decrease. Indeed, the mean particle size dropped from 120 to 4 nm as F decreased from 1000 to 60 J/cm^2, as shown in Fig. 1. In is interesting to note that for lowest ($F < 100$ J/cm^2) and highest ($F > 400$ J/cm^2) fluences the size distributions could easily be extrapolated by Gaussian functions. However, for intermediate fluences between 100 and 400 J/cm^2 the single-peak Gaussian extrapolation was not adequate. An example of such distribution is shown in Fig. 1(b), in which most particles are relatively small with the mean size around 5–10 nm, but a significant number of very large 10–80 nm particles are still present in the solution and the resulting dispersion is rather high. It is known that distributions like these are well described by two Gaussian functions with separated maxima [Fig. 1(b)], suggesting that two different mechanisms are involved in the nanoparticle production. The fluence dependencies of the mean size and dispersion for the relatively narrow (1) and broad (2) distributions are presented in Figs. 2(a) and 2(b). One can see that the peak related to the narrow distribution could be discerned only at $F < 400$ J/cm^2, while the broad distribution-related peak was absent at $F < 100$ J/cm^2. Both distributions demonstrated an increase of the mean size and

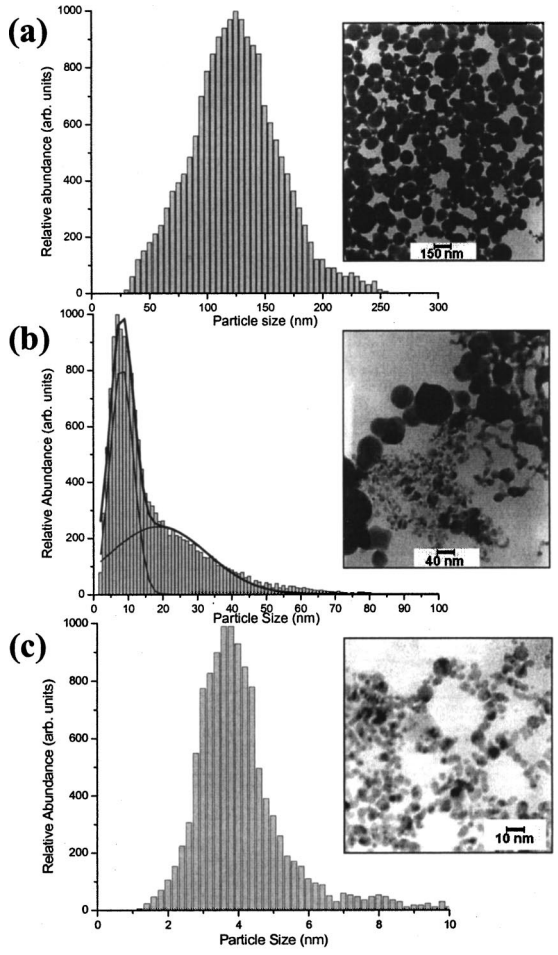

FIG. 1. TEM micrograph images and corresponding size distributions of gold nanoparticles prepared by the femtosecond laser ablation in deionized water at different fluences: (a) 1000 J/cm^2, (b) 160 J/cm^2, and (c) 60 J/cm^2.

dispersion while the fluence increased. However, the increase rate was not very significant for the narrow distribution with ranges of variations for the mean size and dispersion from 4 to 2 nm and from 2 to 17 nm, respectively. In contrast, the broad distribution showed a much stronger and almost linear increase of these characteristics as the fluence increased. Note that the fabrication with nanosecond lasers was accompanied by efficient radiation absorption by the ablated particles suspended in the solution, which provided an additional mechanism of particle reduction.[21] In our conditions this effect was weak or absent since we did not detect any

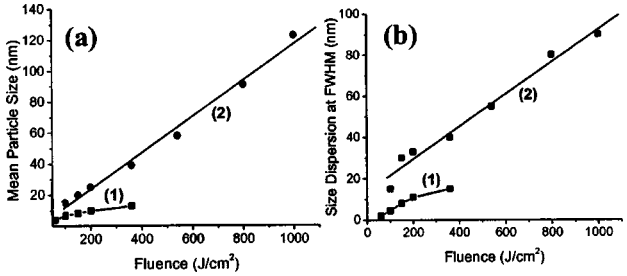

FIG. 2. (a) Mean size and (b) dispersion at FWHM for the narrow (1) and broad (2) distributions of the produced nanoparticles as a function of laser fluence.

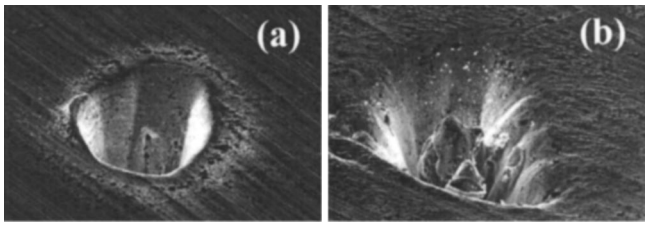

FIG. 3. Typical craters on the gold target in water after 5000 laser pulses at $F=60$ J/cm^2 (a) and $F=1000$ J/cm^2 (b).

difference of the size distributions for samples prepared during different time lengths. Similar weakness of the secondary femtosecond laser ablation of gold particles was mentioned in experiments with chemically prepared colloidal particles.[22] To better understand possible reasons of the particle distribution changes, we performed a SEM study of craters on the gold surface produced by the femtosecond laser ablation in water. As shown in Fig. 3, the craters formed under low and high fluences were quite different. For low fluences Fig. 3(a), the walls of craters were smooth without any indication on the contribution of heating effects. In contrast, the craters prepared at high fluences $F>100$ J/cm^2 [Fig. 3(b)] were broader and had irregular profile, while their walls and bottom contained traces of molten material. In addition, the latter craters were surrounded by a significant heat-affected zone.

It is accepted that the action of laser radiation on a solid target leads to the ablation of material in the form of atoms and nanoscale clusters.[4,5] However, these ablated atoms and clusters tend to aggregate during or after the laser pulse, leading to a formation of much larger particles. In addition, the target itself can be heated by the radiation or by the laser-produced plasma, resulting in the melting and evaporation of the target material and, as a consequence, an ejection of much larger particles. The radiation-related target heating effects are known to be especially strong in cases of microsecond and nanosecond radiations, leading to the appearance of a heat-affected zone surrounding the ablated crater and the ejection of large droplets of the material.[23] In contrast, the action of the femtosecond laser on a solid target is characterized by a significant reduction or a complete removal of this zone as a direct consequence of the laser pulse being much shorter than the heat diffusion time.[23,24] Moreover, with femtosecond radiation, the ablation of material takes place only after the action of the laser pulse, which excludes any additional radiation-related heating of the ablated particles. This later condition should benefit a fast cooling of ablated particles and thus prevent them from the aggregation.

The absence of the heat-affected zone for low fluences [Fig. 3(a)] gives evidence that origin of the narrow distribution is related to the radiative ablation of the target. The surprisingly small mean size (4 nm) and dispersion (2 nm at FWHM) of particles [Fig. 1(c)] are probably granted by the absence of target or particle heating effects during the femtosecond ablation. However, with this mechanism it is difficult to explain the appearance of the additional broad distribution of particles at high fluences [Figs. 1(a) and 1(b)], which was accompanied by the formation of a molten layer on the walls of the crater and around it [Fig. 3(b)]. Taking into account that the target melting cannot result from the radiation-related heating,[24] we propose that the target is heated by the plasma itself. With the lifetime of several microseconds this plasma can become hot enough to ablate the target material, as was previously observed during femtosecond ablation of metals in air.[25] Note that the tendency of the nanoparticle size reduction with the laser fluence decrease was also mentioned under the nanosecond laser ablation of Ag in aqueous SDS solutions.[13] However, with nanosecond pulses the reduction was much weaker (size variations did not exceed 50% of the mean particle size).

In summary, we used a femtosecond laser to ablate a gold target in deionized water and thus fabricate a colloidal solution of gold nanoparticles. We revealed two different nanoparticle distributions, suggesting contributions of different mechanisms of material ablation. The minimal size and dispersion of the produced particles make them very attractive for biosensing applications.

The authors acknowledge the financial contribution from the Natural Science and Engineering Research Council of Canada. We also thank Dr. E. Sacher and J.-P. Sylvestre of Ecole Polytechnique and Dr. J. H. T. Luong of Biotechnology Research Institute (Montreal) for useful discussions.

[1] M. Kerker, The *Scattering of Light and Other Electromagnetic Radiation* (Academic, New York, 1969).
[2] U. Kreibig and M. Vollmer, *Optical Properties of Metal Clusters* (Springer, Berlin, 1996).
[3] *Colloidal Gold: Principles, Methods, and Applications*, edited by M. A. Hyatt (Academic, New York, 1989), Vol. 3.
[4] L. A. Chiu, A. A. Seraphin, and K. D. Kolenbrander, J. Electron. Mater. **23**, 347 (1994).
[5] D. B. Geohegan, A. A. Puretzky, G. Duscher, and S. J. Pennycook, Appl. Phys. Lett. **72**, 2987 (1998).
[6] I. A. Movtchan, R. W. Dreyfus, W. Marine, M. Sentis, M. Autric, G. Le Lay, and N. Merk, Thin Solid Films **255**, 286 (1995).
[7] Y. Yamada, T. Orii, I. Umezu, S. Takeyama, and T. Yoshida, Jpn. J. Appl. Phys., Part 1 **35**, 1361 (1996).
[8] A. V. Kabashin, M. Meunier, and R. Leonelli, J. Vac. Sci. Technol. B **19**, 2217 (2001).
[9] A. V. Kabashin, J.-P. Sylvestre, S. Patskovsky, and M. Meunier, J. Appl. Phys. **91**, 3248 (2002).
[10] A. Fojtik and A. Henglein, Ber. Bunsenges. Phys. Chem. **97**, 252 (1993).
[11] M. S. Sibbald, G. Chumanov, and T. M. Cotton, J. Phys. Chem. **100**, 4672 (1996).
[12] F. Mafune, J.-Y. Kohno, Y. Takeda, T. Kondow, and H. Sawabe, J. Phys. Chem. B **104**, 9111 (2000).
[13] F. Mafune, J.-Y. Kohno, Y. Takeda, T. Kondow, and H. Sawabe, J. Phys. Chem. B **105**, 5144 (2001).
[14] Y.-H. Chen and C.-S. Yeh, Colloids Surf. **197**, 133 (2002).
[15] S. I. Dolgaev *et al.*, Appl. Surf. Sci. **186**, 546 (2002).
[16] T. Tsuji *et al.*, Appl. Surf. Sci. **202**, 80 (2002).
[17] T. Tsuji, T. Kakita, and M. Tsuji, Appl. Surf. Sci. **206**, 314 (2003).
[18] A. V. Kabashin *et al.*, J. Phys. Chem. B **107**, 4527 (2003).
[19] J. Szejtli, in *Comprehensive Supramolecular Chemistry*, edited by J. L. Atwood, J. E. D. Davies, D. D. Macnicol, and F. Vogtle (Pergamon-Elsevier, New York, 1996), Vol. 3.
[20] M. Meunier *et al.*, Proc. SPIE **4978**, 169 (2003).
[21] F. Mafune *et al.*, J. Phys. Chem. **105**, 9050 (2001).
[22] S. Link and M. A. El-Sayed, J. Phys. Chem. B **103**, 8410 (1999).
[23] B. N. Chichkov, C. Momma, S. Nolte, F. von Alvensleben, and A. A. Tunnermann, Appl. Phys. A: Mater. Sci. Process. **63**, 109 (1996).
[24] *LIA Handbook of Laser Materials Processing*, edited by J. F. Ready and D. F. Farson (Springer, Berlin, 2001).
[25] S. M. Klimentov *et al.*, Quantum Electron. **31**, 378 (2001).